

Isotope and surface preparation effects on alkaline dioxygen reduction at carbon electrodes

Jun Xu, Wenhua Huang, Richard L. McCreery *

Department of Chemistry, The Ohio State University, 120 West 18th Ave., Columbus, OH 43210, USA

Received 10 October 1995; in revised form 3 January 1996

Abstract

The reduction of dioxygen in base was examined on several carbon electrode surfaces, particularly polished and modified glassy carbon (GC). Electrochemical pretreatment, fracturing, and vacuum heat treatment shifted the O_2/HO_2^- reduction peak positive, while adsorption of several covalent and physisorbed organic compounds shifted it negative. A reverse wave for O_2^- oxidation was observed in tetraethylammonium hydroxide electrolyte, and on GC surfaces preadsorbed with Co(II) phthalocyanine. An H/D isotope effect was observed when $H_2O + KOH$ and $D_2O + KOD$ electrolytes were compared, with the largest effect observed on surfaces exhibiting the most positive reduction peak potential. The results indicate involvement of proton transfer in the rate limiting step of reduction, and a strong dependence of the O_2/O_2^- electron transfer rate on the carbon surface condition. The results support a mechanism involving adsorption of O_2^- and associated enhancement of proton transfer from water to O_2^- . Activation of the dioxygen reduction by surface pretreatment is attributed to increasing the concentration of adsorbed O_2^- .

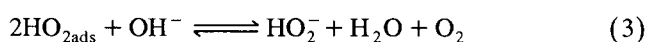
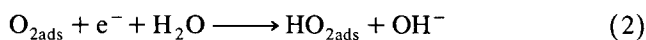
Keywords: Dioxygen; Carbon electrode; Surface preparation; Isotopes; Reduction

1. Introduction

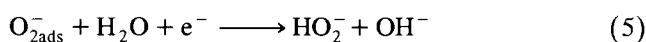
The reduction of dioxygen at carbon based solid electrodes has been a major topic of research both recently and in the past [1–15]. The well known importance of O_2 reduction to water in fuel cells and metal/air batteries has provided the economic driving force for decreasing the O_2 reduction overpotential by electrode modification. Electrocatalysis by carbon supported platinum [16,17], metal macrocycles (e.g. Co and Fe porphyrins) [7,8,18,19], and surface quinones [6,12] has been investigated, as has O_2 reduction on unmodified carbon surfaces [1–5]. Unmodified carbon is of particular interest in alkaline media, in which the first reduction step (to superoxide) occurs in the absence of an added electrocatalyst [10,11]. In practical air cathodes, a carbon electrode modified by a metal macrocycle reduces O_2 to H_2O in a strong base, with the catalyst acting to disproportionate the intermediate HO_2^- [9–11].

The mechanism of O_2 reduction to HO_2^- on carbon in 1 M KOH has been examined several times, but clear agreement on the steps involved has not emerged. Most workers

agree that the first step involves reduction to superoxide, perhaps adsorbed to the carbon surface. In non-aqueous solvents, the O_2/O_2^- couple is chemically reversible with a relatively fast electron transfer rate. There is limited agreement on what occurs after superoxide formation. Morcos and Yeager [4] concluded that a two step reduction of adsorbed O_2 was followed by disproportionation:



Appel and Appleby [2] proposed:



or

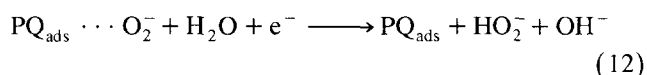
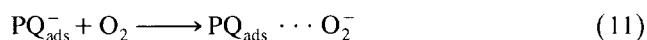


Taylor and Humffray [5] suggested a disproportionation of superoxide:



* Corresponding author.

There are several reports of enhanced O_2 reduction rates at oxidized carbon surfaces, an effect often attributed to catalysis by surface functional groups [11,12]. Redox mediation of O_2 by surface quinones has been considered by several authors, both for adsorbed quinones and quinone functional groups inherent in the carbon surface. Yeager and coworkers [9] have observed O_2 reduction catalysis by adsorbed phenanthrenequinone in base, under conditions where the semiquinone anion (PQ^-) is formed. They propose that adsorbed PQ^- catalyses O_2 reduction on a highly ordered pyrolytic graphite (HOPG) basal plane:



Nagaoka et al. [12] argue that quinone catalysis is possible, but unlikely for oxidized carbon surfaces unmodified by quinone adsorption. They note that O_2 reduction on anodized glassy carbon (GC) is relatively pH independent, while the quinone redox wave shifts at a rate of -68 mV per pH unit. If the quinone mediates the O_2 reduction, then the O_2 wave should also be pH dependent. The same authors also observe [20] that cations interact with the oxidized GC surface in order of increasing strength: $Ba^{2+} < K^+ \approx Na^+ < Li^+$. Although redox mediation by surface quinones is a possibility for O_2 reduction, previous authors do not agree on its importance for the case of oxidized but otherwise unmodified GC surfaces.

Although the mechanistic details of O_2 reduction on carbon remain incomplete, no one doubts that the state of the carbon surface is important. Yeager and coworkers [9] compared O_2 reduction on HOPG and pyrolytic graphite (PG) [9], and Gerischer and coworkers [13,14] compared HOPG and metals in acetonitrile. Disordered carbon materials such as GC have a much higher density of radical and oxide sites than HOPG, and the ordered surfaces may be less able to adsorb O_2 or its reduction products. MacIntyre et al. [14] concluded that surface interactions of O_2^- with a pyrolytic graphite surface resulted in a fundamentally different mechanism from that observed on Hg.

Our laboratory has reported several studies of surface chemical effects on electron transfer at carbon, and we have discussed the importance of carbon microstructure on electrochemical behavior. The majority of the redox systems we considered did not involve adsorption to the carbon surface [21–28], and were controlled by electronic effects in the carbon and inner sphere interactions between redox systems and surface structure. Furthermore, we have described the effects of a variety of surface pretreatments, including laser activation, fracturing, anodization, etc., on outer sphere rates [21–25]. The purpose of the present work is to examine O_2 reduction in base on several carbon surfaces and in several media. Since O_2 reduction is believed to involve adsorption, the effects of carbon pre-

treatment should be pronounced. Our objective is an understanding of the effects of carbon surface structure and electrolyte composition on oxygen reduction kinetics.

2. Experimental

2.1. Electrode preparation

A Bioanalytical Systems GC-20 electrode was conventionally polished with successive 1.0, 0.3, and 0.05 μm alumina slurries prepared from dry alumina and Nanopure water (Barnstead) on a Buehler polishing cloth. The polished electrode was then sonicated in Nanopure water for 5 min before placing it into the electrochemical cell. Although a Kel-f encased polished electrode is not the optimum in terms of reactivity, it served as a convenient starting point for subsequent treatment. Laser activation of the polished electrode was performed by delivering five pulses of an Nd:YAG laser beam operating at 1064 nm onto the electrode surface in the electrolyte under study. The laser power density was 25 MW cm^{-2} , a value which does not yield observable morphological changes to the GC surface [28]. Electrochemical pretreatment (ECP) of the polished electrodes used the procedure of Engstrom and coworker [29,30], involving a 1.8 V potential step (vs. $\text{Ag}|\text{AgCl}$) for 5 min in 0.1 M KNO_3 followed by reduction at -1.0 V for 1 min.

Fractured GC electrodes were prepared as described previously, with fracturing occurring in either Ar or O_2 saturated electrolyte [31]. The typical electrode area was 0.003 to 0.005 cm^2 . HOPG was a gift from Arthur Moore at Union Carbide and was cleaved with an Exacto knife to expose the basal plane. Cyclic voltammetry on HOPG was done using an inverted drop cell [25] and the electrode capacitance was measured by the method of Gileadi [32]. In all cases, the basal plane of HOPG was studied, not the edge plane. Voltammetry was performed in all cases immediately after the surfaces were prepared. In the event of electrode or solution transfer, the electrode surface was kept wet to reduce its exposure to air.

2.2. Electrochemical measurements

Cyclic voltammetry was performed in a custom-designed three-electrode cell. The reference electrode was $\text{Ag}|\text{AgCl}|3 \text{ M KCl}$ with a glass frit and its potential was checked regularly against an SCE to yield a value of 0.203 V vs. SHE. All reported potentials and voltammograms are referenced to this $\text{Ag}|\text{AgCl}$ potential, the auxiliary electrode was a platinum wire. O_2 reduction catalysis did not increase with time, indicating no contamination of the GC with Pt particles from the auxiliary electrode. A triangular waveform triggered by a personal computer was delivered to the electrocell through a conventional three-electrode

potentiostat (Advanced Idea Mechanics, Columbus, OH) with an RC setting according to the criterion $RC\nu < 2$ mV. The electrolyte was saturated with argon (Linde Gas, pre-purified) or oxygen (Linde Gas, ultra-high purity) for 20 min prior to voltammetry. During data acquisition, the purging gas was passed above the solution without disturbing it. Between scans, the solution was further purged with oxygen or argon for 1 min.

2.3. Reagents

All chemicals are of AR grade. 1 M KOH solution was made using pre-boiled Nanopure water and low carbonate KOH pellets (Mallinckrodt). 1 M KOD was made using D_2O (> 99.9 at.% D) and KOD solution (40 wt.% KOD in D_2O , > 98 at.% D) obtained from Aldrich. For electrode area measurements, chronoamperometry of 1 mM $Fe(CN)_6^{3-/4-}$ dissolved in 1 M KCl was used. H_2O_2 (30%, Fisher Scientific) was dissolved in argon saturated KOH or KOD solution and was not analyzed before use, but was approximately 8 mM. All electrolytes were made fresh in Nanopure water and used without pre-electrolysis.

3. Results

The surface exposed by fracturing GC20 in solution is reactive towards outer sphere reactions [23], and has not been exposed to any polishing materials or airborne impurities. The voltammetry of a saturated 1 mM O_2 solution containing 1 M KOH is shown in Fig. 1, along with the background in Ar saturated electrolyte. The peak at ca. -0.3 V vs. Ag|AgCl had a potential $E_{p1} = -0.308$ V vs. Ag|AgCl when the GC electrode was fractured in Ar saturated electrolyte before saturation with O_2 . When the GC was fractured in O_2 saturated KOH, the peak shifted positively ($E_{p1} = -0.289 \pm 0.010$, $N = 4$) and the current of the second peak at ca. -1.0 V increased significantly. ECP further shifted E_{p1} positively ($E_{p1} = -0.234 \pm 0.006$,

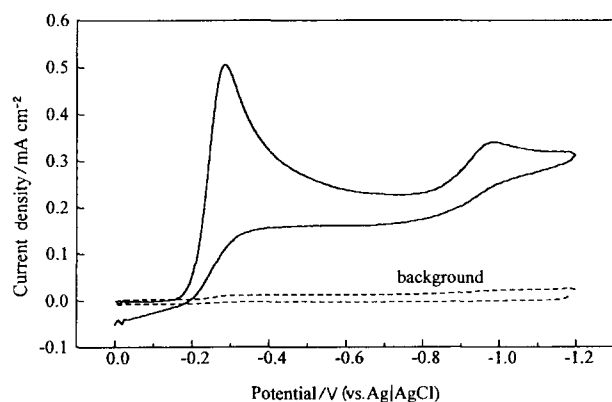


Fig. 1. Voltammograms of 1 M KOH saturated electrolyte at a GC electrode fractured in O_2 saturated electrolyte. Solid line, from a solution saturated with O_2 ; dashed line, after argon saturation at 50 mV s^{-1} .

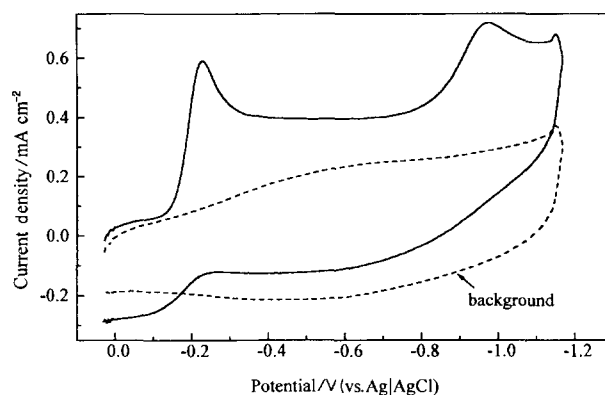


Fig. 2. O_2 voltammetry at an electrochemically pretreated GC electrode, same voltammetric conditions as in Fig. 1.

$N = 5$), and greatly increased the background current (Fig. 2). Background corrected voltammograms for polished, fractured, and electrochemically pretreated of surfaces are compared in Fig. 3, and peak potential data are listed in Table 1. The peak current for peak 1 was linear with $\nu^{1/2}$ for the range 0.02 to 0.20 V s^{-1} .

The voltammetry of O_2 on polished GC is compared with that on the basal plane of HOPG in Fig. 4. The capacitance of HOPG increases for more defective surfaces, so a low capacitance indicates a more perfect basal surface. For the low defect surface ($C^0 = 1.1$ μF cm^{-2}), a significant reduction current was not observed until $E < -0.80$ V. A more defective basal surface ($C^0 = 4.8$ μF cm^{-2}) exhibited more positive peak potentials, but never as positive as that observed on GC. This effect was noted by McIntyre et al. [14] when comparing “ordinary” pyrolytic graphite with HOPG, with the more ordered surface yielding the more negative E_{p1} .

The stoichiometry of the reduction processes can be established with the aid of Figs. 5 and 6. The reduction of HO_2^- (Fig. 5) on an electrochemically pretreated electrode yields a peak at ca. -1.0 V, similar to the second reduction peak of O_2 in KOH. In contrast, the oxidation of HO_2^- exhibited a peak at $+0.60$ V, followed by O_2 reduction at

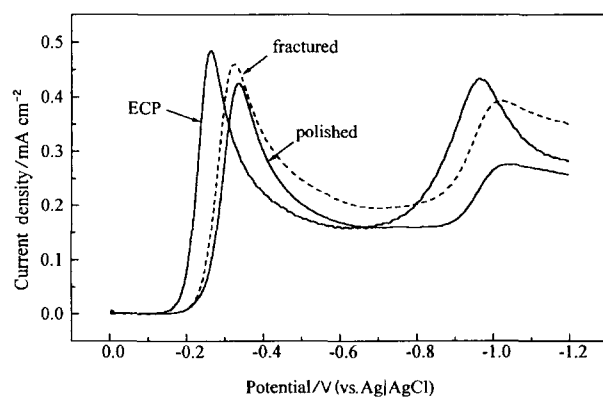


Fig. 3. Comparison of background subtracted voltammograms for O_2 in 1 M KOH at three different GC surfaces, 50 mV s^{-1} .

Table 1
Peak potentials for first O₂ reduction peak^a E_p/V (Ag|AgCl)

	1 M KOH/H ₂ O	1 M KOD/D ₂ O	$\Delta E_{p1}(D-H)$ ^b
Polished	-0.326 ± 0.003 (<i>N</i> = 10)	-0.345 ± 0.008 (<i>N</i> = 2)	-0.019
Fractured/Ar ^c	-0.308 ± 0.008 (<i>N</i> = 2)	-0.325	-0.017
Fractured/O ₂	-0.289 ± 0.010 (<i>N</i> = 4)	-0.312	-0.023
Laser activated (25 MW cm ⁻²)	-0.347 ± 0.015 (<i>N</i> = 5)	-0.369 ± 0.011 (<i>N</i> = 2)	-0.022
ECP in 0.1 M KNO ₃	-0.234 ± 0.006 (<i>N</i> = 5)	-0.268 ± 0.002 (<i>N</i> = 2)	-0.034
Vacuum heat treated	-0.308		

^a Scan rate 0.050 V s⁻¹.

^b (E_{p1} in D₂O) - (E_{p1} in H₂O).

^c Fractured in Ar saturated KOH before O₂ saturation.

ca. -0.4 V on the reverse wave. Such voltammograms are not strongly affected by electrode pretreatments such as ECP. These results confirm previous conclusions [1,15] that the product of the first reduction peak for O₂ is HO₂⁻ under the conditions employed here, and that the reduction peak at -1.0 V is the reduction of HO₂⁻, presumably to H₂O and OH⁻.

It is well known that O₂ reduction is strongly dependent on electrolyte composition, so several variations were examined here. Fig. 7 compares O₂ voltammetry in LiOH, KOH, and TEAOH. Not only does E_{p1} shift in these three electrolytes, but there is a definite reverse wave observable in the case of TEAOH. Sawyer et al. [10] has shown that the O₂/O₂⁻ couple is chemically reversible in TEAP + CH₃CN, although $E_{1/2}$ is substantially more negative (around -0.85 V vs. Ag|AgCl). Although the reverse peaks are fairly broad, it does appear that ECP preceding voltammetry in 1.0 M TEAOH shifts both E_{p1}^a and E_{p1}^c positively, and decreases ΔE_p . A similar but larger effect occurs when Co(II)Pc is adsorbed on the polished surface

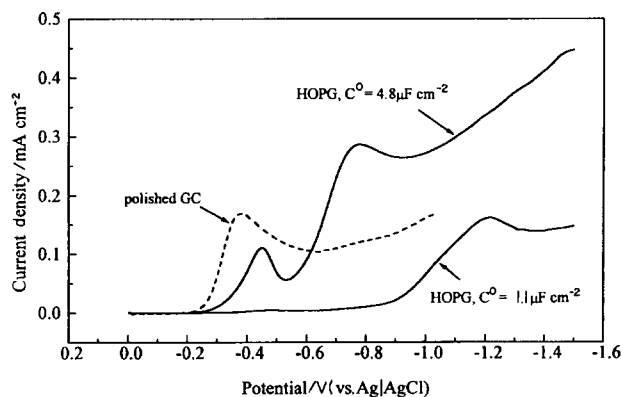


Fig. 4. Voltammograms of O₂ reduction in 1 M KOH on polished GC and basal plane HOPG. Lower HOPG capacitance indicates lower defect density [25].

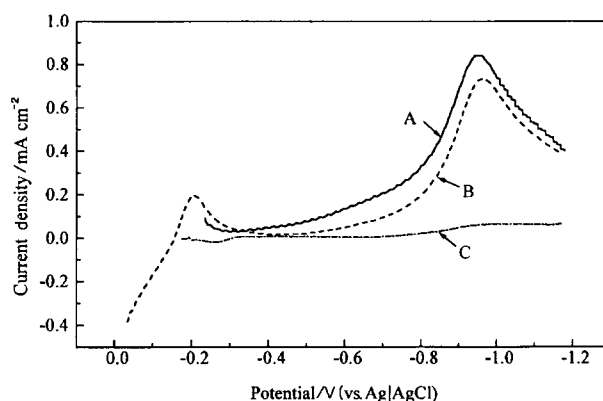


Fig. 5. Reduction of ca. 8 mM HO₂⁻ in 1 M KOH at electrochemically pretreated GC (A and B) and polished GC (C). A and B differ only in their initial potential; scan rate 50 mV s⁻¹.

before voltammetry in 1 M KOH. Both E_{p1}^a and E_{p1}^c shift positively, and ΔE_p decreases to 94 mV.

The involvement of proton transfer steps in the O₂ reduction to HO₂⁻ and H₂O leads to the possibility of hydrogen/deuterium isotope effects on voltammetry. Peak potentials were compared for O₂ reduction and HO₂⁻ oxidation in 1 M KOD/D₂O and 1 M KOH/H₂O, with the results shown in Tables 1 and 2. In all cases, ΔE_{p1D-H} is the shift in peak potential for D₂O compared with H₂O. It was not possible to examine the H/D isotope effect in TEAOH, since the TEAOH is sold as a 2.4 M solution in H₂O.

Several adsorbates were examined for their possible effects on O₂ reduction, with the results listed in Table 3. Anthraquinone 2,6 disulfonate (AQDS) shifted E_{p1} positive relative to the polished surface, as reported for graphite surfaces and attributed to redox mediation [9]. Covalent adsorbates such as dinitrophenylhydrazine (which reacts with surface carbonyls) [33], dinitrobenzoyl chloride (which reacts with surface hydroxyls) [34], and nitrophenylradical

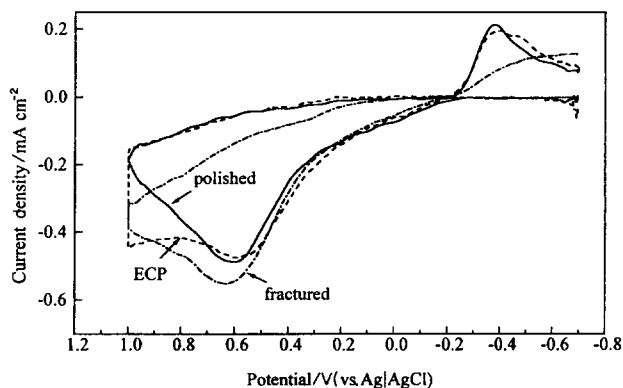


Fig. 6. Voltammetry of ca. 8 mM HO₂⁻ in Ar saturated 1 M KOH on three GC surfaces, 50 mV s⁻¹. Scans were initiated at -0.7 V in a positive direction.

Table 2

Peak potentials for first O₂ reduction peak in several electrolytes (vs. Ag|AgCl)

Polished	E_{p1}^c /V	E_{p1}^a /V	j_{p1} /mA cm ⁻²
1 M TEAOH (polished GC)	-0.350	-0.230	0.28
1 M TEAOH (ECP)	-0.300	-0.186	0.39
2.4 M TEAOH, polished	-0.36	-0.27	
1 M KOH	-0.326		0.40
1 M NaOH	-0.319		0.42
1 M LiOH	-0.310		0.42
1 M KOH + 0.3 mM anthraquinone 2,6 disulfonate			
Polished + DNPH in 1 M KOH	-0.370		0.34
Polished + DNBC in 1 M KOH	-0.380		0.32
Polished + BMB	-0.338	0.116	
ECP (0.1 M KNO ₃)	-0.234		0.53
followed by DNPH	-0.310		
ECP (pretreated and observed in 1 M KOH)	-0.335		

(which non-selectively chemisorbs) [35] all shifted E_{p1} negatively for either the polished or electrochemically pretreated surface. Physisorbed materials such as bismethylstyryl benzene (BMB) [36] had fairly minor, but negative, effects on E_{p1} .

4. Discussion

A mechanism deduced from the experimental results must be consistent with the following observations.

(1) An estimate of the number of electrons in the first reduction from the peak height, assuming an irreversible wave with $\alpha = 0.5$ and $D = 1.75 \times 10^{-5}$ cm s⁻¹, yields $n = 1.9$ to 2.2 for all KOH electrolytes. The value is uncertain in TEAOH owing to possible O₂ solubility differences, but the peak height increases significantly in TEAOH when a polished surface undergoes ECP.

(2) E_{p1} is much more positive for GC than for HOPG, and more positive still if the GC is electrochemically pretreated.

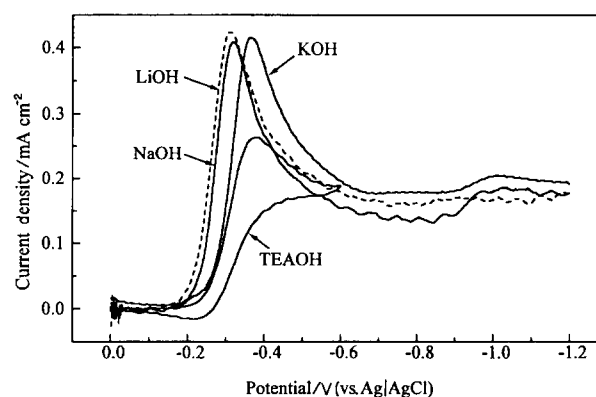


Fig. 7. Effect of electrolyte cation on O₂ reduction on polished GC, 50 mV s⁻¹, saturated O₂ in 1 M concentrations of the electrolytes shown.

(3) Carbon surfaces with the most positive values of E_{p1} show the largest H/D isotope effect.

(4) E_{p1} follows the order Li⁺ ≈ Na⁺ > K⁺ > TEA⁺ for different electrolyte cations.

(5) A reverse wave was observed for the first reduction peak in 1 M and 2.4 M TEAOH, ΔE_p decreased after ECP, and the apparent $E_{1/2}$ shifted positively.

(6) BMB, dinitrophenylhydrazine and dinitrobenzoylchloride adsorptions shift E_p negatively, with oxide specific reagents having the largest effect.

The reverse wave observed at -0.26 V in TEAOH is unlikely to be due to HO₂⁻, since HO₂⁻ oxidation occurs at more positive potentials (Fig. 6). Thus the couple in Figs. 6 and 7 for 1.0 and 2.4 M TEAOH is the quasi-reversible O₂/O₂⁻ couple, with $E_{1/2}$ of approximately 0.31 V vs. Ag|AgCl. E° for the O₂/O₂⁻ couple is strongly medium dependent (ca. -0.8 V in TBAP + CH₃CN) [10], owing to differences in solvation of the O₂⁻ ion. A rough estimate of the apparent electron transfer rate constant for O₂/O₂⁻ can be calculated from ΔE_p for the TEAOH voltammetry (Table 3). Using the classical approach of Nicholson [37], this rate is 0.005 cm s⁻¹. A more rigorous simulation of the voltammetry which confirms this estimate is discussed

Table 3

Simulated voltammetry results for the mechanism of reactions (15)–(18)^a

	k_{15}^0 /cm s ⁻¹	K_{16}	k_{16f} /M ⁻¹ s ⁻¹	E_{p1} /V (Ag AgCl)	j_{p1}^{cath} /mA cm ⁻²	j_{p1}^{anod} /mA cm ⁻²
1	0.005	10 ⁻⁸	100	-0.370	0.287	0.155
2	0.005	10 ⁻⁴	10 ⁴	-0.340	0.478	- ^b
3	0.005	10 ⁻⁴	100	-0.349	0.489	-
4	0.005	10 ⁻⁴	600	-0.344	0.487	-
5	0.1	10 ⁻⁸	100	-0.348	0.310	0.174
6	0.1	10 ⁻⁴	10 ⁴	-0.252	0.609	-
7	0.1	10 ⁻⁴	100	-0.304	0.589	-
8	0.1	10 ⁻⁴	600	-0.283	0.608	-
9	1.0	10 ⁻⁴	100	-0.301	0.600	-
10	1.0	10 ⁻⁴	600	-0.279	0.628	-
Observed in KOH:						
		polished		-0.326	0.44	-
		ECP		-0.234	0.48	-

^a $D_{O_2} = 1.65 \times 10^{-5}$ assuming $D_{O_2} = D_{O_2^-}$, $c_{O_2}^{bulk} = 1.2 \times 10^{-3}$ M, $\nu = 0.05$ mV s⁻¹, $c_{OH^-}^{bulk} = 1.0$ M, $E_1^\circ = -0.310$.

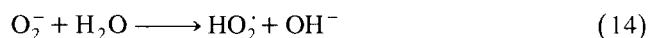
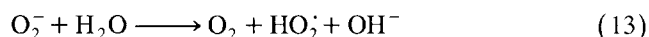
^b Negligible.

below. The j_p vs. $\nu^{1/2}$ linearity of the peak current for the first O_2 reduction peak, and the shape of the O_2/O_2^- couple in TEAOH, do not imply strong adsorption of O_2 or O_2^- but do not rule out weak adsorption.

The O_2/O_2^- couple was concluded to be a quasi-reversible but chemically uncomplicated redox process in acetonitrile and DMSO with ΔE_p on GC of 0.17 V at 0.1 V s⁻¹ [10] and E_p of ca. -0.82 V vs. Ag|AgCl. The more positive $E_{1/2}$ in H₂O [10] compared with CH₃CN was attributed to the larger and more negative solvation energy of O_2^- in H₂O. Yeager and coworkers [38] argued that the O_2/O_2^- is outer sphere but quite slow on HOPG, since there would be no sites for inner sphere catalysis. The fact that k^o is much larger on the GC surface than on HOPG does not necessarily imply that the electron transfer on GC is inner sphere; however, because known outer sphere reactions on GC are generally three to five orders of magnitude slower on the HOPG basal plane [26]. A possible explanation for surface effects on the O_2/O_2^- couple could involve the weak adsorption of O_2^- . Ignoring chemical reactions of O_2^- other than adsorption for the moment, acceleration of k^o by ECP would decrease ΔE_p (as observed in TEAOH). In addition, O_2^- adsorption would shift the apparent $E_{1/2}$ positively, shifting both E_{p1}^c and E_{p1}^a positively, as noted in Table 2. Thus the observed peak potentials in Table 2 (and the simulated values in Table 3, discussed below) do not represent thermodynamic E^o values for O_2/O_2^- , but rather are modified by adsorption and/or subsequent chemical reactions.

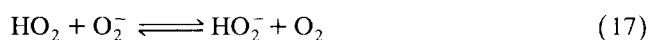
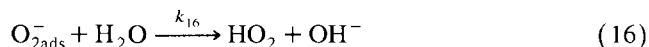
The effect of cation identity on E_{p1} (Fig. 7) could occur either because the cation affects the electron transfer step via an ion pair or double layer interaction, or because the cation modifies chemical steps following O_2^- formation. Sawyer et al. [10] concluded that metal ions facilitated the disproportionation of O_2^- in DMSO to the extent that the O_2/O_2^- couple became irreversible when Zn²⁺ was added to TEAP/DMSO.

After the initial 1e⁻ reduction of O_2 , the second major step involves the fate of O_2^- , adsorbed or not. In solution, reaction (13) is thermodynamically favorable ($K = 1.3 \times 10^6$), but involves an unfavorable proton transfer, reaction (14) ($K = 8 \times 10^{-10}$) [39]:



O_2^- is a relatively weak base, so the forward rate of reaction (14) is at most $K_{14}k_{14b}$, or $8 \text{ M}^{-1} \text{ s}^{-1}$ if the diffusion limit ($k_{14b} = 10^{10}$) is assumed for the reverse of reaction (14). The slow forward rate of reaction (14) is a kinetic bottleneck which retards disproportionation of O_2^- in solution at basic pH.

A key issue is how the electrode surface affects the rate of O_2 reduction to superoxide, and the rate of protonation via reaction (14). As will be shown below, the solution values of $K_{14} = 8 \times 10^{-10}$ and $k_{14f} \leq 8 \text{ M}^{-1} \text{ s}^{-1}$ are too small to explain the observed voltammetry. To undergo the 2e⁻ reduction to HO_2^- , reaction (14) must be accelerated in the presence of the carbon surface. Consider reactions (15)–(18):



or



Reaction (15) is the reduction of O_2 to adsorbed O_2^- , and is quasi-reversible. Based on ΔE_p in TEAOH (where a reverse wave is observable), k_{15}^o is approximately 0.005 cm s^{-1} on polished GC. Reaction (16) is the protonation of O_{2ads}^- , and we propose that K_{16} and k_{16} are increased relative to their solution values by adsorption. Either O_2^- becomes a stronger base upon adsorption, or adsorbed

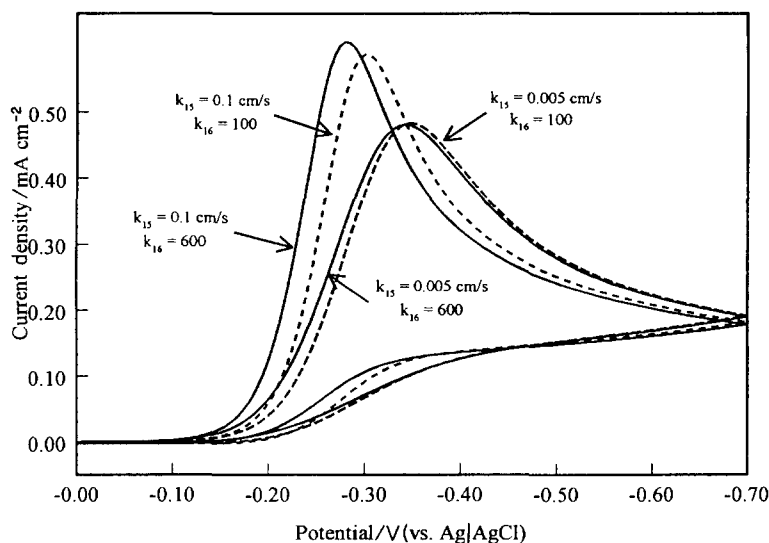


Fig. 8. Simulated voltammograms for O_2 reduction with parameters shown for the mechanism of reactions (15)–(18).

H₂O becomes a stronger acid. The end result is acceleration of reaction (16) when adsorption occurs, compared with reaction (14) in solution. Once HO₂⁻ is formed, it is reduced directly via reaction (18) or indirectly via reaction (17), both of which should be fast.

The H/D isotope effect provides support for this proposed mechanism. If reaction (16) is rate limiting, the H/D rate ratio for reaction (16) should be two to six, and the peak potential should be more negative in KOD/D₂O than in KOH/H₂O. Furthermore, if k_{15} is small, the isotope effect on E_{p1} should be smaller, since reaction (15) would become the rate limiting step. These conjectures are supported by the voltammetry results. The largest isotope effect is observed when E_{p1} is most positive, and reaction (16) is rate limiting (e.g. ECP surfaces). Smaller isotope effects occur when E_{p1} is negative and k_{15}° is small. So the observations indicate a competition between reactions (15) and (16), with their relative rates both depending on surface conditions.

To test the validity of the mechanism represented by reactions (15)–(18), a commercial simulation program [40] was used to predict the effect of variations in rate constants for reactions (15) and (16) on observed voltammetry, with the results shown in Table 3 and Fig. 8. The simulation did not take adsorption into account, but it is useful for determining whether the proposed changes in k_{15}° and k_{16} have the observed effects on E_{p1} . Starting with a k_{15}° of 0.005 cm s⁻¹, simulations 1 and 2 in Table 3 show that large increases in k_{16} and K_{16} have small effects on E_{p1} , although they do double the current. Fig. 8 and simulations 3 and 4 show that an isotope effect involving a factor of six in k_{16} does not greatly affect the voltammetry if k_{15}° is 0.005 cm s⁻¹. However, an isotope effect of 21 mV is observed for $k^{\circ} = 0.1$ (simulations 7 and 8). Stated qualitatively, if k_{15}° is slow enough, the process is limited by reaction (15) and there is no isotope effect. When k_{15}° is fast, the largest isotope effect is observed. As noted experimentally, the largest isotope effects occur when E_{p1} is most positive. We are attributing the more positive E_{p1} to an ECP induced increase in k_{15}° and changes induced in k_{15}° are only sufficient to explain the observed voltammetry at least semi-quantitatively. In order for the simulation to yield an E_{p1} as positive as that observed for the ECP surface, the E° for O₂/O₂⁻ must be adjusted positively, as expected if O₂⁻ adsorbs.

It is apparent from the discussion so far that O₂⁻ adsorption is critical to accelerating reaction (16), and therefore to the production of HO₂⁻. Adsorbates which partially block adsorption, such as BMB, DNPH, etc., decelerate reaction (16) and shift E_p negatively. Increasing the microscopic surface area also increases O₂⁻ adsorption. The ECP surface is known to contain very small graphitic particles and to be permeable by the electrolyte [20]. Enhanced adsorption of O₂⁻ may be responsible for ECP induced catalysis of HO₂⁻ generation. The unexpected behavior of TEAOH electrolyte and the Co(II)Pc modified

surfaces provides additional support for this model. In TEAOH, reaction (16) is slow enough (perhaps because of inhibited adsorption) that O₂⁻ can escape into solution where it is relatively stable. In the case of Co(II)Pc, the generation of O₂⁻ (via reaction (15)) is so fast that O₂⁻ can desorb before protonation. In both cases (fast reaction (15) or slow reaction (16)), enough O₂⁻ enters the solution to be re-oxidized on the reverse scan.

The issue of surface sites inevitably arises when discussing O₂ reduction catalysis on carbon surfaces [1,9,13,38]. Such sites may be surface radicals which adsorb O₂⁻ or they may be oxides which participate in the reaction. It is unlikely that specific oxides could catalyze proton transfer, since they would be deprotonated in 1 M KOH. Oxides may enhance adsorption of O₂⁻ by withdrawing electrons from the surface, a process which would be weakened by DNPH or DNBC derivatization. Whether sites are involved or not, the critical requirement for catalysis is the acceleration of reaction (16) by increasing the pK_a of O_{2ads}⁻ through adsorption. ECP has been shown to generate small carbon particles embedded in the oxide film [41]. The resulting increase in surface area may promote adsorption of O₂⁻ or H₂O.

The mechanism of reactions (15)–(18) is an example of the general EC process, either EC_{cat} if reaction (17) is dominant, or ECE if reaction (18) occurs. Since reaction (17) is a disproportionation, the EC_{cat} mechanism is similar to various disproportionation schemes proposed for other redox systems. Since reactions (17) and (18) are fast compared with reactions (15) and (16), it is difficult to identify with certainty whether (17) or (18) is dominant. The ECP and cation effects indicate that surface and solution conditions alter the relative rates of reactions (15) and (16). Nadjo and Saveant [42] have considered several limiting cases of this general mechanism, in particular a reversible charge transfer and rate limiting chemical step ($E_{rev}C_{ir}$), or a slow charge transfer and fast chemical step ($E_{irr}C_{ir}$). The first O₂ reduction wave is between these limits, shifting from the latter case for a polished surface to the former case for an ECP surface. The HO₂⁻/H₂O peak at ca. -1.0 V vs. Ag|AgCl is less important to possible fuel cell applications due to its negative potential, and is usually bypassed by catalyzing HO₂⁻ disproportionation. Although it was studied in less detail, a few observations are available. First, it is pH dependent, moving positively by 140 mV from pH 14 to 12. Second, it shows a negligible isotope effect on the ECP surface. Third, its behavior is consistent with a slow electron transfer followed by fast chemical steps, leading to H₂O. Overall, the current results do not justify the proposal of a detailed mechanism for HO₂⁻ reduction.

5. Conclusions

The complexity of the O₂ reduction to HO₂⁻ in a base at carbon electrodes results in a variety of possible inter-

pretations of the results. However, two important conclusions are available. First, the pretreatment procedures, particularly ECP, must increase the rate of O₂ reduction to superoxide (k_{15}^0). Second, the existence of an H/D isotope effect on activated surfaces indicates that proton transfer reactions must be comparable in rate to electron transfer ones. Third, adsorption is critical to increasing the reduction rate by accelerating protonation of O₂⁻. Increases in O_{2ads}⁻ from surface pretreatment can be caused either by formation of new adsorption sites or by increases in microscopic surface area. Observed changes in O₂ reduction voltammetry by surface or electrolyte modification can be explained by changes in O₂⁻ adsorption and rate of O₂⁻ generation from O₂.

Acknowledgements

This work was supported by the National Science Foundation and Air Force Office of Scientific Research.

References

- [1] E. Yeager, *J. Mol. Catal.*, 38 (1986) 5.
- [2] M. Appel and A.J. Appleby, *Electrochim. Acta*, 23 (1978) 1243.
- [3] A.J. Appleby and J. Marie, *Electrochim. Acta*, 24 (1978) 1243.
- [4] I. Morcos and E. Yeager, *Electrochim. Acta*, 25 (1979) 195.
- [5] R.J. Taylor and A.A. Humphray, *J. Electroanal. Chem.*, 64 (1975) 63.
- [6] J. Wang, N. Naser, L. Angnes, H. Wu and L. Chen, *Anal. Chem.*, 64 (1992) 1285.
- [7] P.A. Forshey and T. Kuwana, *Inorg. Chem.*, 22 (1983) 699.
- [8] Y.O. Su, T. Kuwana and S.M. Chen, *J. Electroanal. Chem.*, 288 (1990) 177.
- [9] M.S. Hossain, D. Tryk and E. Yeager, *Electrochim. Acta*, 34 (1989) 1733.
- [10] D.T. Sawyer, G. Chlericato, Jr., C.T. Angells, E.J. Nannal, Jr. and T. Tsuchiya, *Anal. Chem.*, 54 (1982) 1720.
- [11] Z.W. Zhang, D.A. Tryk and E. Yeager, in S. Saranganani, J.R. Akridge and B. Schumm (Eds.), *Proc. Workshop on Electrochemistry of Carbon*, The Electrochemical Society, Pennington, NJ, 1984, p. 158.
- [12] T. Nagaoka, T. Sakai, K. Ogura and T. Yoshino, *Anal. Chem.*, 58 (1986) 1953.
- [13] H. Gerischer, R. McIntyre and D. Scherson, *J. Phys. Chem.*, 91 (1987) 1930.
- [14] R. McIntyre, D. Scherson, W. Storek and H. Gerischer, *Electrochim. Acta*, 32 (1987) 51.
- [15] K. Kinoshita, *Electrochemical Oxygen Technology*, Wiley, New York, 1992, Chapter 2.
- [16] W.-H. Kao and T. Kuwana, *J. Am. Chem. Soc.*, 106 (1984) 473.
- [17] H.D. Hutton, N.L. Pocard, D.C. Alsmeyer, O.J.A. Schueller, R.J. Spontak, M.E. Huston, W. Huang, R.L. McCreery, T.X. Neenan and M.R. Callstrom, *Chem. Mater.*, 5 (1993) 1727.
- [18] R.R. Durand, Jr., C.S. Bencosme, J.P. Collman and F.C. Anson, *J. Am. Chem. Soc.*, 105 (1983) 2710.
- [19] J.P. Collman and K. Kim, *J. Am. Chem. Soc.*, 108 (1986) 7847.
- [20] T. Nagaoka et al., *Anal. Chem.*, 60 (1988) 2766.
- [21] M. Poon and R.L. McCreery, *Anal. Chem.*, 58 (1986) 2745.
- [22] R. Rice, C. Allred and R.L. McCreery, *J. Electroanal. Chem.*, 263 (1989) 163.
- [23] R. Rice, N.M. Pontikos and R.L. McCreery, *J. Am. Chem. Soc.*, 112 (1990) 467.
- [24] K.R. Kneten and R.L. McCreery, *Anal. Chem.*, 64 (1992) 2518.
- [25] M.T. McDermott, K. Kneten and R.L. McCreery, *J. Phys. Chem.*, 96 (1992) 3124.
- [26] K.K. Cline, M.T. McDermott and R.L. McCreery, *J. Phys. Chem.*, 98 (1994) 5314.
- [27] R.L. McCreery, K.K. Cline, C.A. McDermott and M.T. McDermott, *Colloid. Surf.*, 93 (1994) 211.
- [28] M.T. McDermott, C.A. McDermott and R.L. McCreery, *Anal. Chem.*, 65 (1993) 937.
- [29] R.C. Engstrom, *Anal. Chem.*, 54 (1982) 2310.
- [30] R.C. Engstrom and V.A. Strasser, *Anal. Chem.*, 56 (1984) 136.
- [31] C.D. Allred and R.L. McCreery, *Anal. Chem.*, 64 (1992) 444.
- [32] E. Gileadi, N. Tshernikovski and M. Babai, *J. Electrochem. Soc.*, 119 (1972) 1018.
- [33] M.A. Fryling, J. Zhao and R.L. McCreery, *Anal. Chem.*, 67 (1995) 967.
- [34] P. Chen, M.A. Fryling and R.L. McCreery, *Anal. Chem.*, 67 (1995) 3115.
- [35] M. Delamar, R. Hitmi, J. Pinson and J.M. Saveant, *J. Am. Chem. Soc.*, 114 (1992) 5883.
- [36] M. Kagan and R. McCreery, *Anal. Chem.*, in press.
- [37] R.S. Nicholson, *Anal. Chem.*, 37 (1965) 1351.
- [38] R.K. Sen, J. Zegal and E. Yeager, *Inorg. Chem.*, 16 (1977) 3379.
- [39] D.T. Sawyer, *Oxygen Chemistry*, Oxford University Press, London, 1991.
- [40] Digisim, *Bioanalytical Systems*, West Lafayette, IN.
- [41] L.J. Kopley and A.J. Bard, *Anal. Chem.*, 60 (1988) 1459.
- [42] L. Nadjo and J.M. Saveant, *J. Electroanal. Chem.*, 48 (1973) 113.